# Theoretical simulation on the Mechanism of Laser Gain Competition in Multi-Order Solid-State Raman Lasers

Jinfang Yang(杨金芳) [1,2], Ke Chen(陈柯)[1], Jieguang Miao(苗杰光)[3*], Qidong Li(李启东)[1], Xinyu Zhan(占昕宇)[1], Weijun Ling(令维军)[1,2*]

*1Gansu Provincial All Solid-State Laser Engineering Research Center, Tianshui Normal University, Tianshui 741001, China;*
*2Engineering Research Center of Integrated Circuit packaging and testing, Ministry of Education, Tianshui 741001, China;*
*3Department of Optoelectronics Science, Harbin Institute of Technology, Weihai Campus, Weihai 264209, China*

To reveal the dynamic characteristics and energy transfer mechanisms of multi-order Raman lasers, we established a set of rate equation groups for first-order, second-order, up to third-order Stokes and first-order Stokes frequency doubling Raman lasers by introducing the rate term of Raman photon number density variation, the spontaneous/stimulated Raman scattering term into the traditional rate equation. Using numerical simulations, we systematically analyzed the dynamic evolution of the intra-cavity population inversion density, as well as the photon number densities of the fundamental frequency laser, each-order Stokes laser, and second-harmonic laser. To address the problem of Raman gain competition caused by multiple orders of Stokes laser sharing the same Raman gain medium and resonator, we proposed a cascaded coupling cavity scheme to suppress this phenomenon, which can provide theoretical basis for achieving high-power and high-spectral-purity Raman laser output.

**Keywords**: rate equations; higher-order Stokes laser; numerical simulation; gain competition

**PACS**:42.55.Yp, 42.55.Rz, 42.65.Dr, 42.55.Ah

## 1.Introduction

Advances in laser technology depend on the expansion into new wavelength bands. Solid-state Raman lasers, which operate on the principle of stimulated Raman scattering (SRS), can achieve efficient output at specific frequencies using various Raman media (such as Nd:$YVO_4$, KTA, and diamond), providing effective solutions for extending laser wavelengths and applications in related fields[1–5]. In recent years, there has been an urgent demand for lasers in the 500–700 nm range in fields such as optical storage, biomedicine, spectroscopic analysis, astronomy, and quantum technology, as well as for lasers in the 1.5–1.6 μm range in fields such as lidar, laser ranging, and environmental monitoring[6–10]. However, conventional solid-state

lasers have limited emission wavelengths that cannot cover these bands, making all-solid-state Raman lasers of significant research value. This is particularly evident in the field of spectroscopy: dual-wavelength (555 nm and 579.5 nm) solid-state Raman lasers can accurately measure carboxyhemoglobin in blood via spectrophotometry[11], while eye-safe 1.5 μm passively Q-switched solid-state Raman lasers also have important applications in laser scanning and spectral analysis[12].

To further expand the wavelength coverage, higher-order Stokes stimulated Raman scattering is an effective approach. Recently, thanks to high-gain Raman media, second- and even third-order Stokes solid-state Raman lasers have been reported [13 – 14]. In 2019, Zhang et al. reported an acousto-optically tuned Q-switched cavity-resonator Nd:YAG/RTP cascaded Raman laser, which ultimately generated higher-order Stokes laser covering the 1000–1200 nm wavelength range, with a total output power of 480 mW and a conversion efficiency of 4.8%[15]. In 2024, Wang et al. used an LD-pumped Nd:YAG/$Cr^{4+}$:YAG bonded crystal to generate 1064 nm fundamental laser, which reduced cavity losses and facilitated the Raman shift toward higher-order Stokes lasers. They then used the 1064 nm laser to pump an RTP Raman crystal, ultimately obtaining a fifth-order Stokes laser at 1244 nm with an average output power of 230 mW, a conversion efficiency of 2.8%, and a slope efficiency of 3.2%[16].

It is evident that, while the multi-order Stokes laser has achieved significant success in extending the wavelength range, the stepwise energy transfer during cascaded oscillation results in a marked decrease in the spectral purity of the Raman laser. This, in turn, further limits the improvement in the power levels and conversion efficiency of each order of Stokes laser. At its root, this issue can be attributed to gain competition in the Raman laser. During their Raman laser experiments, the research group led by H.M. Pask at Macquarie University (Australia) also observed the phenomenon of gain competition in Raman lasers on multiple occasions[17–19]. Therefore, how to theoretically elucidate and overcome this “bottleneck” issue, thereby achieving high-efficiency, high-power Raman laser output, has become an urgent problem to be solved in the current development of solid-state Raman lasers. In 2024, Zhou et al. [20] from Yangzhou University analyzed the cavity structures and parameters of linear and folded cavities using the ABCD transfer matrix method, achieving mode matching between the fundamental laser and the pump laser to reduce the fundamental laser spot size and improve Raman conversion efficiency and output power. In the same year, Li et al.[21] derived theoretical formulas for the optical characteristics of third-order Stokes laser based on the steady-state model of an external-cavity Raman system and effectively simulated the relationships among its key parameters, achieving highly efficient multi-wavelength conversion and control in diamond. Both studies focused on the influence of resonator structure on laser performance. Although they provide theoretical guidance for improving Raman conversion efficiency, they did not explore the fundamental nature of gain competition caused by higher-order coupled oscillations. In 2006, S. Ding et al.[22]

derived a rate equations model for external-cavity Raman lasers and preliminarily established the third-order Stokes rate equations. They explained the consumption of pump laser, as well as the Raman gain and competitive loss of higher-order Stokes laser. However, they did not reveal the time-domain coupling relationships between the population inversion and the photon number densities of each order, making it difficult to guide the suppression of gain competition and the balanced regulation of high-order Raman lasers. Currently, there remains a lack of systematic analysis of rate equations and an explanation of the parameter control mechanisms regarding the gain competition issues caused by cascaded oscillation in high-order solid-state Raman lasers. This is precisely the key factor limiting breakthroughs in the performance of cascaded solid-state Raman lasers.

In this work, by introducing correction terms into the traditional laser rate equation, we established first-order and frequency-doubled, second-order, and third-order Stokes laser rate equations, profoundly revealing the essential laws of the photon density within the cavity and the changes of the optical field. In particular, we explained the mechanism of the gain competition phenomenon existing in multi-order Raman lasers. Finally, we designed an experimental scheme of a cascaded coupled cavity to suppress the gain competition effect, thereby improving the purity of the Raman laser spectrum and the average power.

## 2. Simulation and Design

### 2.1. Derivation of the rate equations for a First-Order Stokes Raman Laser

In general, the rate equations for a laser in the absence of stimulated Raman scattering are as follows [23]:

$$\begin{cases} \dfrac{dn}{dt} = -\gamma\sigma c n\varphi_f - \dfrac{n}{\tau_{sp}} \\ \dfrac{d\varphi_f}{dt} = 2\sigma n l_L \varphi_f \cdot \dfrac{1}{t_{rl}} - \left[ \ln(\dfrac{1}{R_f}) + L_f \right] \cdot \dfrac{\varphi_f}{t_l} + k_f n \end{cases} \tag{2-1}$$

In the equation, $\varphi_f$ is the fundamental-frequency photon number density; $n$ is the population inversion density in the laser medium; $\gamma$ is the decay coefficient for the number of particles; $\sigma$ is the emission cross-section of the laser crystal; $c$ is the speed of laser in a vacuum; $\tau_{sp}$ is the lifetime of the upper energy level of the laser crystal; $l_L$ is the length of the laser crystal; $t_{rl}$ is the round-trip time of the fundamental laser within the cavity; $R_f$ is the reflectance of the output mirror pair for the fundamental frequency laser; $L_f$ is the round-trip diffraction loss of the fundamental laser within the cavity; $k_f$ is the proportion of photons in spontaneous emission that correspond to the stimulated oscillation mode; $t_l$ is the photon lifetime of the fundamental-frequency laser.

The specific expression for $t_l$ is as follows:

$$t_l = \frac{t_{rl}}{\ln(\dfrac{1}{R_f R_s}) + L_f + L_Q} \tag{2-2}$$

In the equation, $L_Q$ is the Q-factor.

Since the value of the fundamental-frequency photon lifetime $t_l$ is long, it is neglected in the calculations presented in this paper.

In (2-1), the left-hand side of the first equation represents the rate of change of the population inversion density with respect to time; the first term on the right-hand side represents the decrease in population inversion caused by laser emission resulting from the transition of atoms from high-energy levels to lower-energy excited levels, while the second term represents the decrease in population inversion caused by spontaneous emission. Since this term is small, its effect can be neglected in numerical simulations.

In (2-1), the left-hand side of the second equation represents the rate of change of the photon number density in the cavity over time. The first term on the right-hand side represents the increase in photon number density due to stimulated emission, while the second term represents the decrease in radiation caused by system losses in the optical resonator. The primary causes of system losses include transmission and absorption at the end mirrors, diffraction losses due to the finite aperture of the mirrors, and scattering and absorption losses inherent to the laser material itself. The third term represents the increase in photon number density due to spontaneous emission; however, because its magnitude is small, it is often neglected in calculations. In the numerical simulations conducted in this paper, since spontaneous emission and spontaneous Raman scattering are weak and have a negligible impact on the solution of the rate equations, all terms related to spontaneous emission and spontaneous Raman scattering are neglected in the calculations.

Next, we will discuss the derivation of the first-order Stokes Raman laser rate equations. Under the plane-wave approximation, the expressions for the laser rate equations are as follows:

$$\begin{cases} \dfrac{dn}{dt} = -\gamma\sigma c n\varphi_f - \dfrac{n}{\tau_{sp}} \\ \dfrac{d\varphi_f}{dt} = 2\sigma n l_L \varphi_f \cdot \dfrac{1}{t_{rl}} - 2g_1 h\nu_f c l_s \varphi_f \varphi_{s1} \cdot \dfrac{1}{t_{rs}} - \left[\ln(\dfrac{1}{R_f}) + L_f\right] \cdot \dfrac{\varphi_f}{t_l} + k_f n \\ \dfrac{d\varphi_{s1}}{dt} = 2g_1 h\nu_f c l_s \varphi_f \varphi_{s1} \cdot \dfrac{1}{t_{rs}} - \left[\ln(\dfrac{1}{R_f}) + L_f\right] \cdot \dfrac{\varphi_{s1}}{t_{s1}} + k_f \varphi_f \end{cases} \tag{2-3}$$

In the equation, $\varphi_{s1}$ is the first-order Stokes photon number density; $\nu_f$ is the frequency of the fundamental laser; $l_s$ is the length of the Raman crystal; $t_{rs}$ is the round-trip time of first-order Stokes Raman laser within the cavity; $R_s$ is the reflectance of the output mirror for Raman laser; $L_s$ is the round-trip diffraction loss of Raman laser within the cavity; $t_{s1}$ is the first-order Stokes Raman photonic lifetime; $k_s$ is the proportion of photons in spontaneous Raman scattering that correspond to the stimulated oscillation mode; a typical value is $10^{-3}$[24].

Compared to the second equation in (2-1), the second equation in the set of rate equations (2-3) has the same left-hand side, which represents the rate of change in the fundamental-frequency photon number density. However, the right-hand side includes an additional term, $(-2g_1 h\nu_f c l_s \varphi_f \varphi_{s1})/t_{rs}$, which accounts for the coupling between the fundamental laser and the Raman laser to generate the first-order Stokes laser. The negative sign preceding this additional term indicates that the fundamental laser is consumed during this process. The left-hand side of the third equation in the rate

equations system (2-3) represents the rate of change of the first-order Stokes Raman photon number density with respect to time. The first term $(2g_1 h\nu_f c l_s \varphi_f \varphi_{s1})/t_{rs}$ on the right-hand side of the equation represents the increase in the first-order Stokes Raman photon number density following stimulated Raman scattering. Since this increase in the Raman photon number density results from the coupling between the fundamental laser and the Raman laser—at the expense of the fundamental laser—therefore, the absolute values of the $(-2g_1 h\nu_f c l_s \varphi_f \varphi_{s1})/t_{rs}$ term in the second equation of the system (2-3) and the $(2g_1 h\nu_f c l_s \varphi_f \varphi_{s1})/t_{rs}$ term in the third equation are equal. The second term on the right-hand side of the third equation represents system loss, while the third term represents the portion of photons in spontaneous Raman scattering that correspond to the stimulated oscillation mode.

### 2.2. Derivation of the rate equations for a First-Order Stokes Second-Harmonic Raman Laser

The laser rate equations are a theoretical model that describes the variation of the population inversion density and photon density. By numerically solving the rate equations using MATLAB software to simulate the dynamic characteristics of the fundamental laser, first-order Stokes laser, and first-order Stokes second-harmonic laser, it is possible to develop strategies for increasing the output pulse energy and conversion efficiency. Based on the rate equations for a first-order Stokes Raman laser and using the plane-wave approximation, a set of rate equations for a first-order Stokes second-harmonic Raman laser has been established. The specific expressions are as follows:

$$\begin{cases} \dfrac{dn}{dt} = -\gamma\sigma c n\varphi_f - \dfrac{n}{\tau_{sp}} \\ \dfrac{d\varphi_f}{dt} = 2\sigma n l_L \varphi_f \cdot \dfrac{1}{t_{rl}} - 2g_1 h\nu_f c l_s \varphi_f \varphi_{s1} \cdot \dfrac{1}{t_{rs}} - [\ln(\dfrac{1}{R_f}) + L_f] \cdot \dfrac{\varphi_f}{t_l} + k_f n \\ \dfrac{d\varphi_{s1}}{dt} = 2g_1 h\nu_f c l_s \varphi_f \varphi_{s1} \cdot \dfrac{1}{t_{rs}} - [\ln(\dfrac{1}{R_f}) + L_f] \cdot \dfrac{\varphi_{s1}}{t_{s1}} - \left|\dfrac{d\varphi_{s1}}{dt}\right| SHG + k_s \varphi_f \\ \dfrac{d\varphi_h}{dt} = \left|\dfrac{d\varphi_{s1}}{dt}\right| SHG - [\ln(\dfrac{1}{R_h}) + L_h] \cdot \dfrac{\varphi_h}{t_h} \end{cases} \quad (2\text{-}4)$$

In this equation, $\varphi_h$ represents the photon density of the second-harmonic laser.

The specific expression for the first term on the right-hand side of the fourth equation in the system of rate equations (2–4) is as follows:[25]:

$$\left|\frac{d\varphi_s}{dt}\right| SHG = \frac{1}{4}\rho\eta h\nu_s \frac{c^2}{L_c}\varphi_s^{\,2} \quad (2\text{-}5)$$

(2-5) In this equation, $\rho$ represents the mode-overlap factor, $\eta$ represents the frequency-doubling conversion efficiency, expressed as follows:

$$\eta = 2(\frac{\mu}{\varepsilon})^{1/2} \frac{\omega^2 d_{eff}^{\,2} l_h^{\,2}}{n_1^{\,2} n_2 c^2} \frac{\sin^2(l_h \Delta k/2)}{(l_h \Delta k/2)^2} \quad (2\text{-}6)$$

In this equation, $\mu$ is the magnetic permeability in a vacuum; $\varepsilon$ is the dielectric constant; $\omega$ is the angular frequency of the first-order Stokes laser; $d_{eff}$ is the nonlinear coefficient of the second-harmonic generation crystal; $l_h$ is the length of the second-harmonic generation crystal; $n_1$ is the refractive index of the fundamental

laser in the medium; $n_2$ is the refractive index of the second-harmonic laser in the medium; and $\Delta k$ is the mismatch constant.

### 2.3. Derivation of the rate equations for a Second-Order Stokes Raman Laser

Based on the rate equations for a first-order Stokes Raman laser, the rate equations for a second-order Stokes Raman laser have been derived. The specific expressions are as follows [26]:

$$\begin{cases} \dfrac{dn}{dt} = -\gamma\sigma c n\varphi_f - \dfrac{n}{\tau_{sp}} \\ \dfrac{d\varphi_f}{dt} = 2\sigma n l_L \varphi_f \cdot \dfrac{1}{t_{rl}} - 2g_1 h\nu_f c l_s \varphi_f \varphi_{s1} \cdot \dfrac{1}{t_{rs}} - \left[\ln(\dfrac{1}{R_f}) + L_f\right] \cdot \dfrac{\varphi_f}{t_l} + k_f n \\ \dfrac{d\varphi_{s1}}{dt} = 2g_1 h\nu_f c l_s \varphi_f \varphi_{s1} \cdot \dfrac{1}{t_{rs}} - 2g_2 h\nu_{s1} c l_s \varphi_{s1} \varphi_{s2} \cdot \dfrac{1}{t_{rs2}} - \left[\ln(\dfrac{1}{R_f}) + L_f\right] \cdot \dfrac{\varphi_{s1}}{t_{s1}} + k_f \varphi_f \\ \dfrac{d\varphi_{s2}}{dt} = 2g_2 h\nu_{s1} c l_s \varphi_{s1} \varphi_{s2} \cdot \dfrac{1}{t_{rs2}} - \left[\ln(\dfrac{1}{R_f}) + L_f\right] \cdot \dfrac{\varphi_{s2}}{t_{s2}} \end{cases} \tag{2-7}$$

In the equation, $\varphi_{s2}$ is the second-order Stokes photon number density; $g_1$ , $g_2$ are the Raman gain coefficients of the $BaWO_4$ crystal at the fundamental frequencies of 1064 nm and 1180 nm; $\nu_{s1}$ , $\nu_{s2}$ are the frequencies of the 1180 nm and 1325 nm Raman lasers in the $BaWO_4$ crystal; $t_{rs1}$ , $t_{rs2}$ are the round-trip times of the first- and second-order Raman laser in the cavity; $t_{s1}$ , $t_{s2}$ are the photon lifetimes of the first- and second-order Raman laser.

Compared to the rate equations set (2-3), the third equation in the rate equations set (2-7) includes an additional term $(-2g_2 h\nu_{s1} c l_s \varphi_{s1}\varphi_{s2})/t_{rs2}$ on the right-hand side. The physical significance of this term is that first-order Stokes Raman laser acts as the "pump laser" to generate second-order Stokes Raman laser; the negative sign preceding the expression indicates that the first-order Raman laser is being consumed. The left-hand side of the fourth equation represents the rate of change of the second-order Stokes photon number density with respect to time; the first term $(-2g_2 h\nu_{s1} c l_s \varphi_{s1}\varphi_{s2})/t_{rs2}$ on the right-hand side represents the newly generated second-order Stokes Raman laser, while the second term represents system losses.

### 2.4. Derivation of the rate equations for a Third-Order Stokes Raman Laser

Based on the rate equations for a second-order Raman laser, the rate equations for a third-order Raman laser are derived as follows:

$$\begin{cases} \dfrac{dn}{dt} = -\gamma\sigma c n\varphi_f - \dfrac{n}{\tau_{sp}} \\ \dfrac{d\varphi_f}{dt} = 2\sigma n l_L \varphi_f \cdot \dfrac{1}{t_{rl}} - 2g_1 h\nu_f c l_s \varphi_f \varphi_{s1} \cdot \dfrac{1}{t_{rs}} - \left[ \ln(\dfrac{1}{R_f}) + L_f \right] \cdot \dfrac{\varphi_f}{t_l} + k_f n \\ \dfrac{d\varphi_{s1}}{dt} = 2g_1 h\nu_f c l_s \varphi_f \varphi_{s1} \cdot \dfrac{1}{t_{rs}} - 2g_2 h\nu_{s1} c l_s \varphi_{s1} \varphi_{s2} \cdot \dfrac{1}{t_{rs2}} - \left[ \ln(\dfrac{1}{R_s}) + L_s \right] \cdot \dfrac{\varphi_{s1}}{t_{s1}} + k_f \varphi_f \\ \dfrac{d\varphi_{s2}}{dt} = 2g_2 h\nu_{s1} c l_s \varphi_{s1} \varphi_{s2} \cdot \dfrac{1}{t_{rs2}} - 2g_3 h\nu_{s2} c l_s \varphi_{s2} \varphi_{s3} \cdot \dfrac{1}{t_{rs3}} - \left[ \ln(\dfrac{1}{R_s}) + L_s \right] \cdot \dfrac{\varphi_{s2}}{t_{s2}} \\ \dfrac{d\varphi_{s3}}{dt} = 2g_3 h\nu_{s2} c l_s \varphi_{s2} \varphi_{s3} \cdot \dfrac{1}{t_{rs3}} - \left[ \ln(\dfrac{1}{R_s}) + L_s \right] \cdot \dfrac{\varphi_{s3}}{t_{s3}} \end{cases} \tag{2-8}$$

In the equation, $\varphi_{s3}$ represents the rate of change of the third-order Stokes photon number density with respect to time; $g_3$ represents the Raman gain coefficient of the $BaWO_4$ crystal at the second-order Stokes Raman wavelength of 1325 nm; $t_{rs3}$ represents the round-trip time of the third-order Raman laser within the cavity; $t_{s3}$ represents the photon lifetime of the third-order Raman laser.

The fourth equation in the system of rate equations (2–8) includes an additional term $(-2g_3 h\nu_{s2} c l_s \varphi_{s2} \varphi_{s3})/t_{rs3}$ compared to the fourth equation in (2–7); this term represents the portion of the second-order Stokes Raman laser that is consumed as "pump laser" to generate third-order Stokes Raman laser. The left-hand side of the fifth equation represents the rate of change of the third-order Stokes photon number density with respect to time. The first term $(2g_3 h\nu_{s2} c l_s \varphi_{s2} \varphi_{s3})/t_{rs3}$ on the right-hand side represents the newly generated third-order Stokes Raman laser, the absolute value of which equals the consumed second-order Stokes Raman laser, while the second term represents system losses.

## 3. Analysis and Discussion

### 3.1. Numerical Simulation Results and Analysis of a First-Order Stokes Raman Laser

Using the ODE45 function in MATLAB to solve the first-order Stokes Raman laser rate equations, we numerically simulated the dynamic changes in the photon density and population inversion density within the cavity, as well as the pulse shape and width, thereby revealing the dynamic behavior of the fundamental and Raman lasers. The parameter values required for solving the first-order Stokes Raman laser rate equations are shown in Table 1.

The numerical simulation results for the rate equations of a first-order Raman laser are shown in Figure 1. Figure 1(a), Figure 1(b), and Figure 1(c) show the corresponding pulse shapes and the trends in the fundamental laser, Raman laser, and population inversion densities for Raman cavity lengths of 80 mm, 140 mm, and 225 mm, respectively. In Figure 1, the blue line represents the curve of the population inversion density as a function of time, the green line represents the curve of the fundamental laser photon density as a function of time, and the red line represents the curve of the first-order Stokes Raman laser photon density as a function of time.

The Nd: $YVO_4$ laser crystal is a medium with a four-level system. When the pump

laser is sufficiently intense, particles in the ground state are pumped into a higher energy level. Because this higher energy level is unstable, the particles rapidly relax to the upper laser level, at which point the upper laser level achieves population inversion. The particles then transition from the upper laser level to the lower laser level, emitting laser in the process, while the particles in the lower laser level rapidly transition back to the ground state without emitting radiation. In this process, the generation of laser light occurs at the expense of the population inversion.

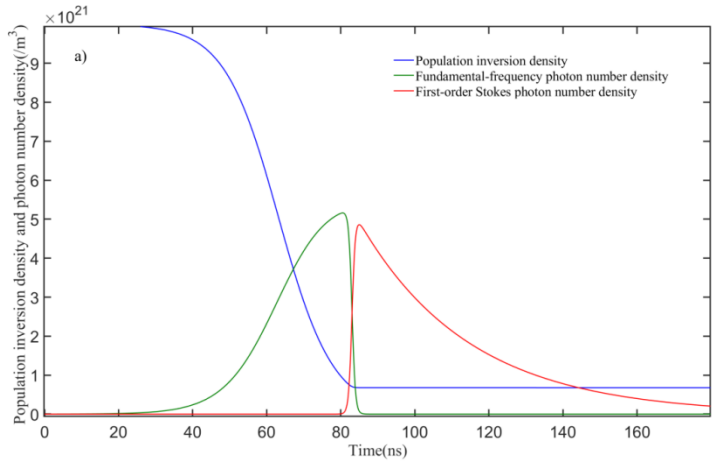
As shown in Figure 1, the decreasing population inversion is used to generate the fundamental-frequency laser; as the population inversion continues to decrease—that is, as it is depleted—the photon density of the fundamental-frequency laser gradually increases. When the intensity of the fundamental laser is sufficiently high, stimulated Raman scattering occurs, generating first-order Stokes Raman laser. This explains why the rising edge of the fundamental laser pulse in Figure 1 is relatively gentle, while the falling edge is steep and decays rapidly. Figure 1 also shows that the first-order Stokes Raman laser begins to develop only after the fundamental laser has been established for some time, reflecting the threshold nature of Raman laser generation. Furthermore, while the fundamental laser decays rapidly, the Raman laser begins to develop rapidly, demonstrating that the generation of Raman laser occurs at the expense of the fundamental laser's photon count. Only when the Raman gain is greater than the total loss within the cavity, can the Stokes photons be continuously amplified, enabling the output of laser oscillation.

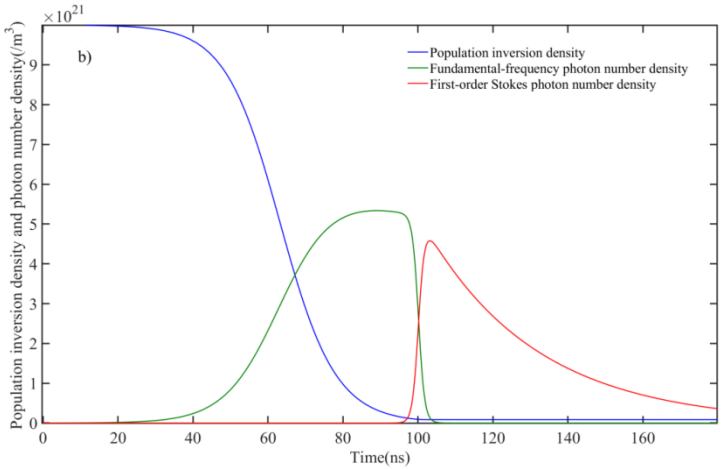
**Table 1** Resonator parameters used in solving the rate equations

| physical quantity | Parameters | numerical value |
|---|---|---|
| Stimulated emission cross section($m^2$) | $\sigma$ | $7.6\times10^{-23}$ |
| speed of laser (m/s) | c | $2.998\times10^{8}$ |
| Planck constant | $\hbar$ | $1.05\times10^{-34}$ |
| Fundamental optical wavelength (nm) | $\lambda_f$ | 1064 |
| First-order Stokes wavelength (nm) | $\lambda_{s1}$ | 1180 |
| Second-order Stokes wavelength (nm) | $\lambda_{s2}$ | 1325 |
| Third-order Stokes wavelength (nm) | $\lambda_{s3}$ | 1510 |
| Raman shift ($cm^{-1}$) | $\Delta\upsilon$ | 925 |
| First-order Stokes Raman gain coefficient(m/W) | $g_1$ | $8.5\times10^{-11}$ |
| Second-order Stokes Raman gain coefficient(m/W) | $g_2$ | $7.57\times10^{-11}$ |
| Third-order Stokes Raman gain coefficient(m/W) | $g_3$ | $6.64\times10^{-11}$ |
| Fundamental mode cavity loss | $L_l$ | 0.01 |
| Raman cavity loss | $L_s$ | 0.01 |
| Laser crystal length (mm) | $l_L$ | 5 |

| | | |
|---|---|---|
| Raman crystal length (mm) | $l_S$ | 30 |
| Output mirror reflectance for fundamental frequency laser | $R_f$ | 0.99 |

As shown in Figure 1(a), when the Raman cavity length is short (80 mm), the rising edge of the Raman laser pulse (i.e., the red solid line) is steeper, indicating that the photon density of the Raman laser increases rapidly. The first-order Raman scattering is very strong, and the Raman laser pulse establishes too quickly, preventing the energy of the inverted population from being fully converted into fundamental-frequency laser. This results in a residual inverted population that is not conducive to increasing the pulse energy. As shown in Figure 1(b), when the Raman cavity length (140 mm) increases, the steepness of the pulse rise time decreases relative to Figure 1(a), the photon density increases more slowly, and the first-order Raman scattering effect becomes relatively weaker. As shown in Figure 2(c), when the Raman cavity length is further increased to 225 mm, the rise time of the pulse becomes even more gradual compared to Figures 3-1a and 3-1b, the increase in photon density slows down further, and the first-order Raman scattering becomes too weak. The first-order Stokes laser only begins to build up after the fundamental laser photon density has decreased for a period of time. Consequently, the fundamental laser photons cannot be fully utilized, resulting in the loss of a significant number of them.



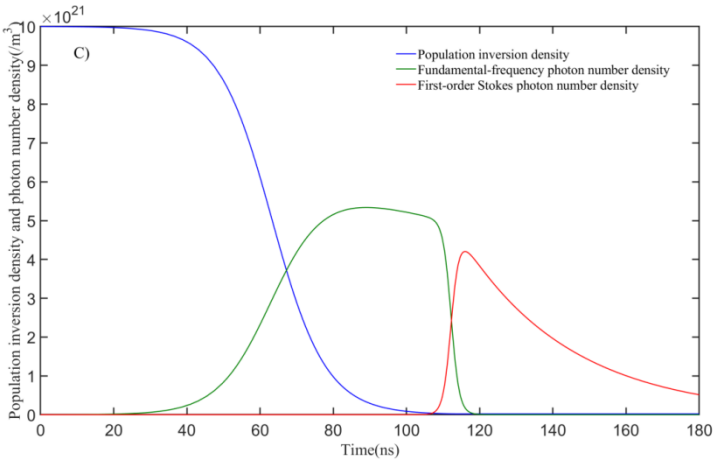



**Fig. 1.** Variation of population inversion density, fundamental-frequency photon number density and first-order Stokes photon number density in the cavity with cavity length

a) 80 mm b) 140 mm c) 225 mm

### 3.2. Numerical Simulation Results and Analysis of a First-Order Stokes Second-Harmonic Raman Laser

The numerical simulation results for the first-order Stokes-doubled Raman laser are shown in Figure 2. Compared to Figure 1, the trends in the population inversion density and the fundamental-frequency photon number density remain essentially unchanged, with the addition of a black curve. This black curve represents the rate of change of the first-order Stokes-doubled laser photon density over time. When the first-order Stokes Raman laser begins to build up, the second-harmonic laser also begins to build up simultaneously. There is no time delay in the generation of the second-harmonic laser relative to the Raman laser, indicating that as long as Raman laser is generated, second-harmonic laser will also be generated, demonstrating the threshold-free nature of the second-harmonic laser. Compared to the first-order Stokes laser, the pulse width of the second-harmonic laser is narrower. Furthermore, the falling edge of the first-order Stokes Raman laser pulse in Figure 1 is relatively gentle, with a slow decay, whereas the falling edge in Figure 2 is steeper, with a rapid decay. This is because the first-order Stokes Raman laser is consumed as “pump laser” to generate the second-harmonic laser. The essence of intracavity frequency doubling is that two first-order Stokes photons directly convert into a frequency-doubled photon by a nonlinear medium, without the need to satisfy the oscillation conditions. Therefore, the frequency-doubled laser has no threshold characteristic.

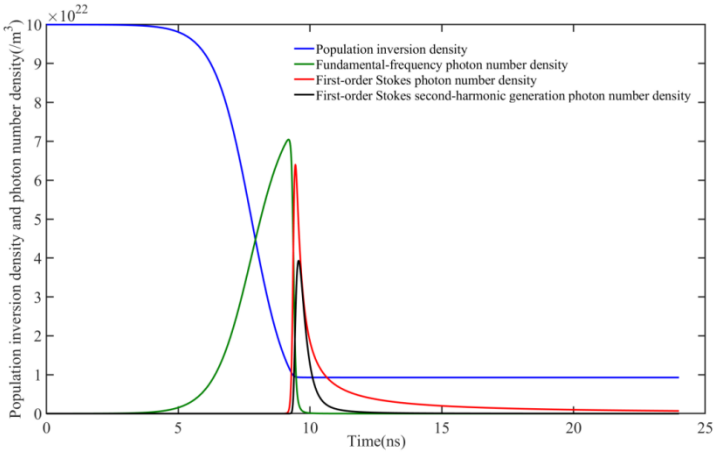


**Fig. 2.** Variation of population inversion density, fundamental-frequency photon number density, first-order Stokes photon number density, and first-order Stokes second-harmonic generation photon number density in the cavity.

### 3.3. Numerical Simulation Results and Analysis of a Second-Order Stokes Raman Laser

The rate equations for a second-order Stokes Raman laser were solved numerically, and the simulation results are shown in Figure 3. The solid yellow line in the figure represents the second-order Stokes photon number density. The figure shows that the pulse width of the first-order Raman laser decreases relative to that of the fundamental laser, and as the inversion population of the laser crystal is depleted, the fundamental laser begins to build up. Only after the fundamental laser has been established for some time does the first-order Stokes Raman laser begin to establish itself. Since the fundamental laser serves as the pump laser for the first-order Stokes Raman laser, it decays rapidly. The first-order Stokes Raman laser, in turn, acts as a "pump laser" to generate the second-order Stokes Raman laser, so it also decays rapidly. The second-order Stokes Raman laser begins to establish only after the first-order Stokes Raman laser has been established for some time, which again demonstrates the threshold nature of Raman laser generation. Additionally, there is a certain time delay in the establishment of the first-order Stokes Raman laser relative to the fundamental laser, and of the second-order Stokes Raman laser relative to the first-order Stokes Raman laser pulses, reflecting the threshold characteristics of the Raman laser generation process.

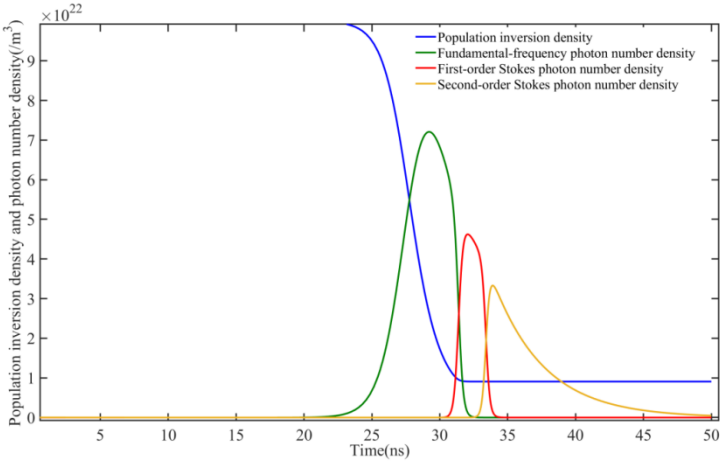



**Fig. 3.** Variation of population inversion density, fundamental-frequency photon number density, first-order Stokes photon number density, and second-order Stokes photon number density in the cavity

### 3.4. Numerical Simulation Results and Analysis of a Third-Order Stokes Raman Laser

The numerical simulation results for the third-order Raman laser are shown in Figure 4, which primarily discuss the time evolution of the population inversion density and the photon number densities of the fundamental laser, first-order, second-order, and third-order Stokes lasers within the cavity. In the figure, the blue line represents the population inversion density, the green line represents the fundamental-frequency photon number density, the red line represents the first-order Stokes photon number density, the yellow line represents the second-order Stokes

photon number density, and the purple line represents the photon density of the third-order Stokes photon number density.

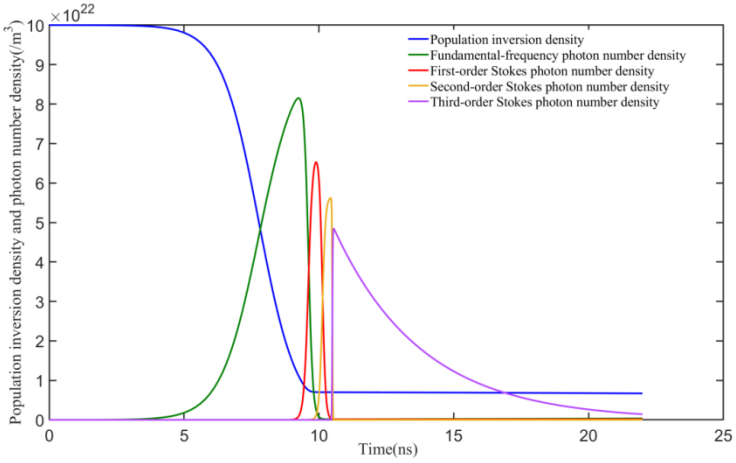



**Fig. 4.** Variation of population inversion density, fundamental-frequency photon number density, first-order Stokes photon number density, second-order Stokes photon number density, and third-order Stokes photon number density in the cavity

As shown in Figure 4, first-order Stokes Raman laser serves as the pump laser to generate second-order Stokes Raman laser, which in turn serves as the pump laser to generate third-order Stokes Raman laser, demonstrating the cascading oscillation characteristics of higher-order stimulated Raman scattering. Consequently, the first- and second-order Stokes Raman laser decays rapidly, and their pulse widths are significantly compressed relative to that of the fundamental laser pulse. Furthermore, since the photon density of the pump laser inside the cavity is very low when third-order Stokes Raman laser is generated, it is difficult to reach the pump power threshold required for third-order Stokes generation; consequently, the third-order Stokes Raman laser is relatively weak, and the corresponding pulse width is relatively broad. This figure also illustrates the dynamic characteristics of the medium's inversion particle number density and the changes in the photon density within the cavity.

### 3.5 Design of an experimental scheme to suppress Raman gain competition

When the fundamental pump power density is extremely high, the Raman laser will generate a cascade effect of higher-order Stokes laser, with energy transferred step by step, the higher-order Stokes laser shares the same resonator and Raman crystal. This causes each order of Stokes laser to occupy and consume the ground-state particle population of the Raman crystal, leading to a gain competition effect. To address this, we have designed a novel coupled-cavity structure that allows each order of Stokes laser to obtain sufficient gain in independent Raman media and relatively independent resonators. Combined with selective feedback from the cavity mirror system, this approach effectively resolves such gain competition issues.

In this experiment, a LD (Laser Diode) with a central wavelength of 880 nm was used to pump a 1064 nm Nd: $YVO_4$ laser. The 1064 nm laser cavity was used to pump a $BaWO_4$ crystal, and the 925 $cm^{-1}$ frequency shift peak of the crystal was utilized to achieve efficient oscillation of the third-order Stokes laser (1510 nm), thereby resolving the gain competition issues between it and the first-order Stokes laser (1180 nm) and the second-order Stokes laser (1325 nm).The experimental setup is shown in Figure 5, where $M_1$, $M_{S1}$, and $M_2$ form the 1064 nm fundamental-frequency optical resonator. $M_2$ and $M_3$ form the 1180 nm Raman optical resonator. $M_3$, $M_{S1}$, $M_{S2}$, and $M_4$ form the 1325 nm Raman optical resonator; and $M_4$ and $M_5$ form the 1510 nm

Raman optical resonator. Within the same Raman crystal, only the pump laser and its corresponding Stokes laser exist, and there is no problem of higher-order Stokes laser "taking over" the ground-state particles of the Raman crystal. Theoretically, this structure can also be periodically expanded to achieve higher orders of Stokes laser oscillations.

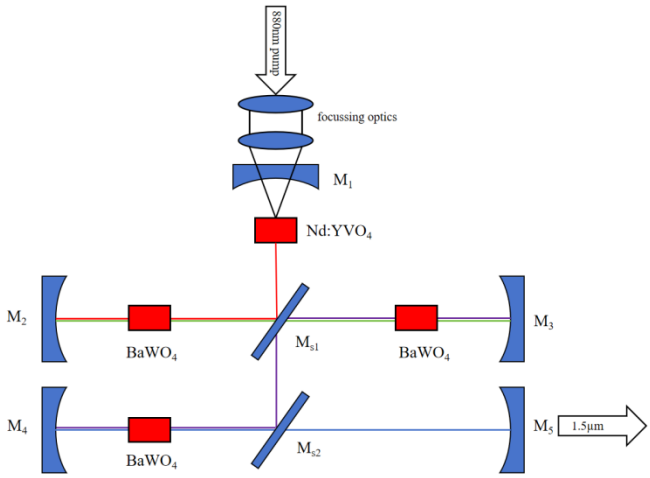



**Fig. 5.** Experimental scheme design for suppressing Raman gain competition.

## 4. Conclusion

We established a set of rate equations for first-, second-, and third-order Stokes laser and first-order Stokes-doubled Raman lasers, and analyzed their dynamic characteristics, energy transfer mechanisms, and gain competition mechanisms. The key conclusions are as follows: (1) The first to third-order Stokes effects exhibit significant threshold characteristics, and the establishment of each order of Stokes laser involves a time delay. The cavity length can effectively regulate the energy conversion efficiency of Raman scattering. (2) The frequency-doubled laser exhibits a threshold-free oscillation characteristic and has shorter pulse duration. (3) The energy is successively transferred among different orders of Raman laser, and the conversion efficiency is significantly affected by the number of cascades. (4) Considering that the shared resonant cavity and the Raman medium are the fundamental causes of gain competition, we initially propose a coupling cavity structure suppression scheme, which can effectively solve such gain competition problems.

## Acknowledgement

This work was supported by National Natural Science Foundation of China (Grant Nos. 62405221), Gansu Province College Industry Support Plan Project (Grant No.2024CYZC-44), the Natural Science Foundation of Gansu Province (Grant Nos. 25JRRE009), National Key R&D Program Key Special Project: R&D of Key Materials and Devices for National Quantum Science and Technology (No. 2025YFH0101002), Tianshui Strong Science and Technology Award special project (TS-STK-2024A-277),
Gansu Province University Postgraduate Innovation Star Project of Tian-shu i Normal University (No. 2026CXZX-987)

## References

[1] Mi X B, Ma H J, He J R, Yang X, Cheng L W, Zhang Y, Wang J Q, Hu Y S and Shan C X 2025 Opt. Laser Technol. 187 112843
[2] Ma H J, Mi X B, He J R, Ma F Y, Yang X, Zhang Y, Cheng L W, Hu Y S and Shan C X 2025 Opt. Laser Technol. 189 113157
[3] Fan L, Zhao X D, Zhang Y C, Gu X D, Wan H P, Fan H B and Zhu J 2019 Chin. Phys. B 28(8) 188
[4] Zhu H Y, Shao Z H, Wang H Y, Duan Y M, Zhang J, Tang D Y and Kaminskii A A 2014 Opt. Express 22(16) 19662
[5] Xu J J, Zhang X Y, Cong Z H, Liu Z J, Chen X H, Qin Z G, Gao F L, Wang P, Wang Z C and Ming N 2020 Chin. J. Lasers 47(6) 42
[6] Lin X J, Ren H K, Wang Z P, Li Y, Sun X and Xu X G 2025 Opt. Laser Technol. 186 112697
[7] Xing T, Xing E B, Jia T, Li J L, Rong J M, Zhou Y R, Liu W Y, Tang J and Liu J 2022 Chin. Phys. B 31(10) 488
[8] Huang H J, Fang Y H, Chen C L, Liang H C and Chen Y F 2023 Opt. Lett. 48(17) 4645
[9] Savitski V G, Reilly S and Kemp A J 2015 Conference on Lasers and Electro-Optics Europe CA_8_4
[10] Huang Y J, Chen Y F, Chen W D and Zhang G 2015 Opt. Lett. 40(15) 3560
[11] Chen Y F, Chang X W, Lin S Q, Huang H J, Hsieh L W and Liang H C 2024 Opt. Express 32(17) 30335
[12] Zhang H, Zhang N H, Xin D, He H K, Xu J H, Zhou X Y, Zheng W H and Zhang H B 2025 Opt. Lett. 50(7) 2137
[13] Lin J P and Pask H M 2012 Opt. Express 20(14) 15180
[14] Lin H Y, Pan X, Huang X H, Xiao M, Liu X, Sun D and Zhu W Z 2016 Opt. Commun. 368 39
[15] Zhang J, Duan Y M, Zhang D, Zhang Y C, Wang H Y and Zhu H Y 2019 Infrared Laser Eng. 48(6) 346
[16] Wang J, Jin X X, Wang Y Y, Wang H Y, Li Z H, Duan Y M and Zhu H Y 2024 High Power Laser Part. Beams 36(6) 58
[17] Lee A J, Pask H M, Piper J A, Zhang H and Wang J 2010 Opt. Express 18(6) 5984
[18] Yu H H, Li Z, Lee A J, Li J, Zhang H J, Wang J Y, Pask H M, Piper J A and Jiang M H 2011 Opt. Lett. 36(4) 579
[19] Lin J and Pask H M 2012 Appl. Phys. B 108(1) 17
[20] Zhou A W, Sun X C, Wang Y, Yue Y F, Xiang K Y, Shen J and Fan L 2024 Electron. Dev. 47(4) 968
[21] Li X W, Chen H, Cui Y F, Ding J, Qi Y Y, Yan B Z, Wang Y L, Lü Z W and Bai Z X 2024 Acta Opt. Sin. 44(22) 162
[22] Ding S, Zhang X, Wang Q, Su F, Li S, Fan S, Zhang S, Chang J, Wang S and Liu Y 2006 Appl. Phys. B 85(1) 89
[23] Li S, Dong Y, Jin G and Lü Y 2015 Infrared Laser Eng.
[24] Ding S, Zhang X, Wang Q, Chang J, Wang S and Liu Y 2007 IEEE J. Quantum Electron. 43(8) 722

[25] Cong Z H, Zhang X Y, Wang Q P, Liu Z J, Chen X H, Fan S Z, Zhang X L, Zhang H J, Tao X T and Li S T 2010 Opt. Express 18(12) 12111
[26] Ding S H 2006 Theoretical and Experimental Research on All-Solid-State Raman Lasers (Ph.D. Dissertation) (Jinan: Shandong University)